



In Situ Synthesis and Photocatalytic Properties of Titanium Dioxide Nanoparticles on Cotton Fabrics

Zhanxia Bao · Shuhua Wang · Xiaoying Yu ·
Yindong Gao · Zeling Wen

Received: 27 March 2019 / Accepted: 27 June 2019 / Published online: 9 July 2019
© Springer Nature Switzerland AG 2019

Abstract In this paper, nanosized titanium dioxide as catalysts for degrading dye wastewater was in situ synthesized on the surface of cotton fabrics used tetrabutyl titanate as precursor. The morphology and structure of prepared catalysts were characterized by scanning electron microscopy, energy-dispersive spectrometer, and X-ray diffraction. The characterization results showed that anatase nanosized titanium dioxide was successfully synthesized in situ on cotton fabrics and had excellent dispersibility. Subsequently, the effects of irradiation time, catalyst dosage, dye concentration, initial pH value of dye, hydrogen peroxide dosage, and dye type on dye degradation rate were investigated one by one by a photocatalytic performance test. The test results indicated that the degradation rates of methylene blue, methyl orange, and rhodamine B were 90.4%, 81.4%, and 58.3%, separately, at catalyst dosage of 4.8 g/L, initial dye concentration of 10 mg/L, pH of 7, and hydrogen peroxide dosage of 0.24 mol/L, after 4 h of UV irradiation.

Highlights In this work, anatase nanosized titanium dioxide composite materials with high degradation performance to various types of dyes were prepared via an orthogonal design-oriented low-temperature calcination of waste cotton fabrics.

- (1) The introduction of orthogonal experiment could be efficient, fast, and economical in optimizing experimental parameters.
- (2) Titanium dioxide with high dispersibility could endow the cotton fabrics striking degradation performance to dyes.
- (3) Recycling and reusing waste fabrics could be significant for relieving resource shortage, saving energy, and reducing emission.

Z. Bao · S. Wang (✉) · X. Yu · Y. Gao · Z. Wen
College of Textile Engineering, Taiyuan University of
Technology, Taiyuan 030600, People's Republic of China
e-mail: wangshuhua@tyut.edu.cn

Keywords Dye wastewater · Tetrabutyl titanate · Titanium dioxide · Cotton fabrics · Photocatalytic performance · Degradation rate

1 Introduction

As a kind of semiconductor material with efficient photocatalytic activity, nanosized titanium dioxide (nano-TiO₂) possesses nontoxicity, high chemical stability, and excellent photocatalytic activity (Zhou et al. 2017; Goudarzi and Shahabi-Ghahfarrokhi 2018). Due to its attractive properties, nano-TiO₂ could be widely applied in a variety of fields such as sterilization, air purification, and water treatment (Wang et al. 2015; Zhang et al. 2017). However, nano-TiO₂ also has some disadvantages. First of all, the disadvantage of easy agglomeration of nano-TiO₂ greatly limits its performance. Due to the large specific surface area and high surface energy of pure nano-TiO₂ particles, which belong to thermodynamic unstable systems, the surface particles cluster together with each other due to van der Waals force and Coulomb force, so that the nano-TiO₂ particles are agglomerated and lose the physical properties and functions when applied. Therefore, it is imperative to prepare highly dispersed nano-TiO₂ to maintain its advantages in photocatalytic performance. Secondly, nano-TiO₂ particles in the water system are easy to lose, difficult to recycle, and high in recycling cost (Liu et al. 2018). Therefore, it is necessary to find a suitable carrier to immobilize nano-TiO₂ for recycling. In order to solve

the above problems, many scholars have extensively studied supported nano-TiO₂ photocatalysts.

At present, the carrier materials commonly loading nano-TiO₂ mainly include silicas (Sosnov et al. 2017), polymers (Vukoje et al. 2016), glasses (Yusoff et al. 2016), and carbon materials (Das et al. 2018; Xu et al. 2016a, b; Liang et al. 2018). All these materials have the characteristics of good stability, high strength, large specific surface area, and firm load. Because of large surface area, interwoven network structure of yarns, inherent strength, and flexibility, the cotton fabrics (CFs) can provide a good bearing platform for nano-TiO₂, which is conducive to the formation of highly dispersed TiO₂, thus maximizing its dye degradation performance. At the same time, TiO₂ also provides a choice to impart multifunctional properties of the CFs (Mishra and Butola 2017; Giesz et al. 2016).

The annual output of waste CFs is huge, and they cannot be used reasonably, which will not only pollute the environment but also waste resources greatly (Pensupa et al. 2017). Therefore, using CFs as the carrier of TiO₂ not only has a wide source and low cost but also protects the environment and makes effective utilization of resources (Ma et al. 2018). As reported by Giesz et al., using the methods of sol-gel process and microwave treatment successfully prepared TiO₂-anatase film on cotton and viscose fabric surfaces (Giesz et al. 2016).

In this work, nano-TiO₂ synthesized in situ and loaded on CFs was successfully prepared by using a hydrothermal method and low-temperature calcination, with cheap and readily available CFs as carrier and tetrabutyl titanate (TBT) as raw material. The loaded nano-TiO₂ had anatase crystal form, high dispersion, and superior catalytic activity.

2 Experiments

2.1 Raw Materials and Reagents

CFs were used as substrate for loading nano-TiO₂. Nano-TiO₂ was prepared from TBT as raw material. The dyes, methylene blue (MB), methyl orange (MO), and rhodamine B (RhB) are all of analytical reagent (AR) grade and are commercially available.

2.2 Preparation of Loaded-TiO₂ Cotton Fabrics (TiO₂/CFs)

According to the analysis of this experiment, there are many factors affecting photocatalytic degradation rate,

such as hydrolysis temperature, hydrolysis time, hydrothermal temperature, hydrothermal time, calcination temperature, calcination time, dye type, dye concentration, solution pH value, illumination time, illumination intensity, and hydrogen peroxide (H₂O₂) dosage. After comprehensive consideration, the hydrolysis temperature, hydrothermal temperature, hydrothermal time, and calcination time were determined as the experimental factors for the preparation of the experiment and were marked as *A*, *B*, *C*, and *D*, respectively. Three-level and four-factor orthogonal experiments were carried out. The factors and levels are shown in Table 1.

The specific preparation process of the experiment was as follows: 1.6 g CFs were immersed in 8 mL TBT for 24 h at room temperature, followed by taking out the CFs and squeezing away as much liquid as possible from the surface of the CFs. Then, loaded TBT CFs were quickly immersed into 20 mL deionized water to hydrolyze for 30 min. Subsequently, it was transferred to a polytetrafluoroethylene autoclave for hydrothermal treatment. After a certain period of time, the products were poured into a beaker, washed three times with deionized water (to remove unloaded or not firmly loaded TiO₂ particles from the CFs surface), and dried at 60 °C. Finally, the products were calcined at 200 °C and cooled to obtain TiO₂/CFs. A simulation of the preparation process is shown in Fig. 1.

2.3 Photocatalytic Degradation of MB, MO, and RhB under UV Irradiation

MB, MO, and RhB were selected as model chemicals to evaluate the photocatalytic performance of TiO₂/CFs. About 0.30 g of TiO₂/CFs was placed separately in 60 mL of MB, MO, and RhB solution (10 mg/L). Before irradiation, these solutions were stirred (500 r/min) in the dark for 30 min to achieve the adsorption equilibrium (Wu and Long 2011). Then, they were exposed to UV radiation with the wavelength of 365 nm (UV-365) maintaining

Table 1 Factors and levels of orthogonal design

Levels	Experimental factors			
	<i>A</i> /°C	<i>B</i> /°C	<i>C</i> /h	<i>D</i> /h
1	60	120	6	2
2	80	150	8	3
3	100	180	10	4

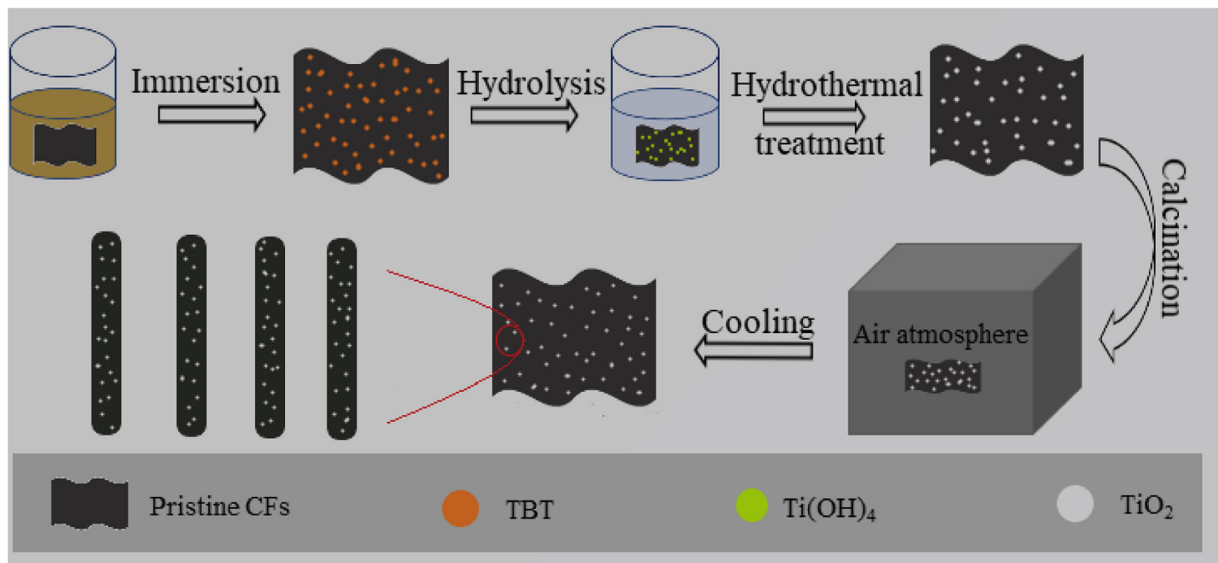


Fig. 1 The preparation of TiO₂/CFs

vigorous stirring (500 r/min). The MB, MO, and RhB solutions were taken out at regular intervals, and the absorbances were measured by a 721 visible spectrophotometer, at the maximum absorption wavelength of 664 nm (Phaltane et al. 2017), 464 nm (John et al. 2017), and 552 nm (Cai et al. 2018), respectively. Before measuring, the suspensions were filtered through an organic micropore filter (pore size 0.45 μm). Taking MB solution as an example, since the MB solution concentration *C* (mg/L) was proportional to the absorbance within a certain range as shown in Fig. 2, it could be approximately expressed as (Eq. (1)):

$$A = 0.12057C, R^2 = 0.99883. \tag{1}$$

Therefore, the degradation rate *D*(%) could be calculated by replacing the concentration *C* with the absorbance *A*. Eventually, the degradation rate was calculated by the measured absorbance as follows (Eq. (2)) (Zhang and Yang 2012):

$$D = [(A_0 - A_t) / A_0] \times 100\% \tag{2}$$

where *A*₀ is the absorbance of the MB solution after dark reaction for 30 min; *A*_{*t*} is the absorbance of the MB solution irradiated for *t*.

3 Results and Discussions

3.1 Orthogonal Test

This experiment was a three-level and four-factor test, where only the effect of the four factors on the degradation rate was considered, ignorance of the interactions among the factors. Therefore, *L*₉ (3⁴) orthogonal table should be selected. The specific test conditions and results are shown in Table 2. The degradation rates of MB evaluated and recorded as *D*_{MB}, as the final evaluation index.

As shown in Table 2, the orders for the average values (\bar{K}) of each factor were as follows: $\bar{K}_{A2} > \bar{K}_{A1} > \bar{K}_{A3}$, $\bar{K}_{B2} > \bar{K}_{B1} > \bar{K}_{B3}$, $\bar{K}_{C3} > \bar{K}_{C1} > \bar{K}_{C2}$, and $\bar{K}_{D1} > \bar{K}_{D3} > \bar{K}_{D2}$. Therefore, *A*₂, *B*₂, *C*₃, and *D*₁ could be determined as the optimal levels of factors *A*, *B*, *C*, and *D*, respectively. The combination of *A*₂*B*₂*C*₃*D*₁ was the optimal level combination in this experiment. This meant that the optimal preparation conditions were hydrolysis temperature 80 °C, hydrothermal temperature 150 °C, hydrothermal time 10 h, and calcination time 2 h. The range (*R*) calculation demonstrated that *R*_{*B*} > *R*_{*D*} > *R*_{*A*} > *R*_{*C*}. Hence, for MB, the greatest influence was hydrothermal temperature, followed by calcination time and hydrolysis temperature, while hydrothermal time was the least influence.

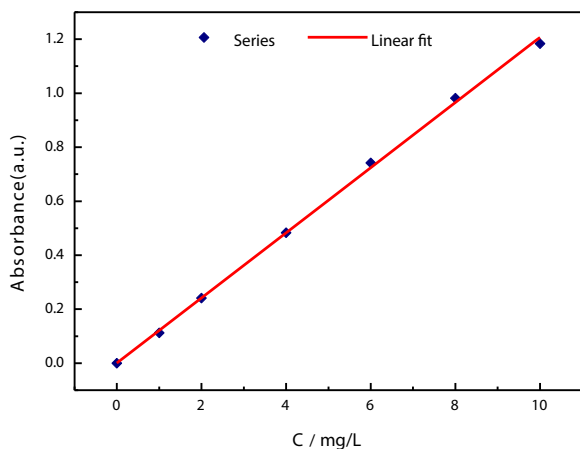


Fig. 2 Standard working curve of MB solution

3.2 Characterization of Morphology and Structure

3.2.1 Scanning Electron Microscopy and Energy-Dispersive Spectrometer

Scanning electron microscopy (SEM) was used to characterize the surface morphology of the samples and the distribution of TiO₂ particles on CFs as shown in Fig. 3. The chemical composition of TiO₂/CFs was characterized by energy-dispersive spectrometer (EDS) as shown in Fig. 4.

Table 2 Specific test conditions and results

Sample	A (°C)	B (°C)	C (h)	D (h)	D _{MB} (%)
1	60	120	6	2	30.8
2	60	150	8	3	32.3
3	60	180	10	4	26.3
4	80	120	8	4	29.4
5	80	150	10	2	37.7
6	80	180	6	3	24.8
7	100	120	10	3	27.3
8	100	150	6	4	32.3
9	100	180	8	2	25.4
K ₁	89.4	87.5	87.9	93.9	
K ₂	91.9	102.3	87.1	84.4	
K ₃	85.0	76.5	91.3	88.0	
⁻ K ₁	29.8	29.2	29.3	31.3	
⁻ K ₂	30.6	34.1	29.0	28.1	
⁻ K ₃	28.3	25.5	30.4	29.3	
R	2.3	8.6	1.4	3.2	

Figure 3a is a SEM image of the original CFs, from which it could be observed that the surface had a small amount of natural impurities and warp (Yang et al. 2019), so it had a certain roughness and was beneficial to the loading of TiO₂. Figure 3b is a SEM image of TiO₂/CFs, from which it could be observed that CFs still maintained its original shape, and TiO₂ was uniformly and firmly distributed on the surface of the CFs. This was because there were many free hydroxyl groups on the surface of CFs, which could react with hydroxyl radicals (-OH) on the surface of TiO₂, so the combination between them was strong enough. Through EDS energy spectrum analysis, it could be found that the prepared TiO₂/CFs contained C, Ti, and O elements, which further confirmed the in situ synthesis of TiO₂ on CFs.

3.2.2 X-Ray Diffraction

X-ray diffraction (XRD) was carried out to determine the crystal structure (brookite, anatase, or rutile) of TiO₂ particles on CFs at 2θ from 10° to 70° with Cu Kα radiation, as shown in Fig. 5. Figure 5a showed the XRD pattern of the pristine CFs as blank samples, from which only the characteristic peaks of CFs were observed. Figure 5b shows the XRD pattern of the prepared TiO₂/CFs, from which not only the characteristic diffraction peaks 15.6°, 16.8°, and 23.1° of CFs but also the characteristic diffraction peaks 25.6°, 38.2°, 48.2°, 54.3°, and 62.2° of typical anatase TiO₂ were observed, corresponding to the crystal faces of (101), (112), (200), (211), and (204) (Sun et al. 2000; Zhou et al. 2017). In addition, using the XRD diffraction pattern of Fig. 4b, the crystallite diameter (*D*) of anatase TiO₂ crystal was calculated based on (101) crystal face reflection according to the Scherer formula (Eq. (3)) (Kinsinger et al. 2011; Sun et al. 2000):

$$D = k\lambda / (\beta \cos\theta) \quad (3)$$

where *k* is the shape constant (typical around 0.9) (Tang et al. 2009), λ is the wavelength of the Cu Kα radiation (λ = 0.154 nm), β is the full width at half maximum (FWHM), and θ is the diffraction angle. The TiO₂ particle size was about 9.4 nm. Therefore, TiO₂ was a nanosized particle.

From above, it could be determined that in situ synthesis of anatase nano-TiO₂ particles on CFs could be achieved by the hydrothermal method and low-temperature (200 °C) calcination. Therefore, in order

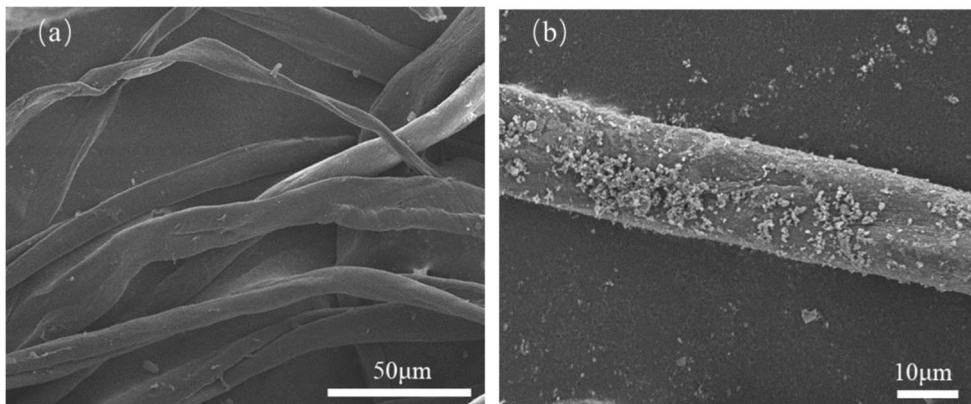


Fig. 3 SEM images of the two samples. **a** Pristine CFs. **b** TiO₂/CFs

to make use of the photocatalytic properties of nano-TiO₂, the prepared TiO₂/CFs would be used in the research of dye-simulated wastewater treatment in the subsequent work.

3.3 Photocatalytic Degradation Performance

3.3.1 Effects of UV Irradiation Time on Photocatalytic Activity

Figure 6 shows the effects of irradiation time on photocatalytic performance of TiO₂/CFs under the conditions of UV-365 irradiation, MB solution concentration of 10 mg/L, and TiO₂/CFs dosage of 4.8 g/L. As can be seen from Fig. 6, the degradation rate of pristine CFs to MB solution in 9 h under UV-365 irradiation was about

15%, which was basically negligible in comparison with the higher degradation rate of TiO₂/CFs. For TiO₂/CFs, the degradation efficiency of MB solution gradually decreased with the increase of irradiation time, but the degradation rate gradually increased. This was because the intermediate products produced in the process of MB degradation occupied the active parts of TiO₂, and a competition for degradation may occur between the MB and the intermediate products (Rauf et al. 2011), resulting in a decrease in degradation efficiency. Especially after 5 h, the degradation efficiency of MB solution was only 1.6%. However, with the gradual reaction of intermediate products and the continuous adsorption and degradation of MB solution, the degradation rate showed an increasing trend. However, after 5 h, the degradation rate also tended to be basically balanced.

Fig. 4 EDS energy spectrum of TiO₂/CFs

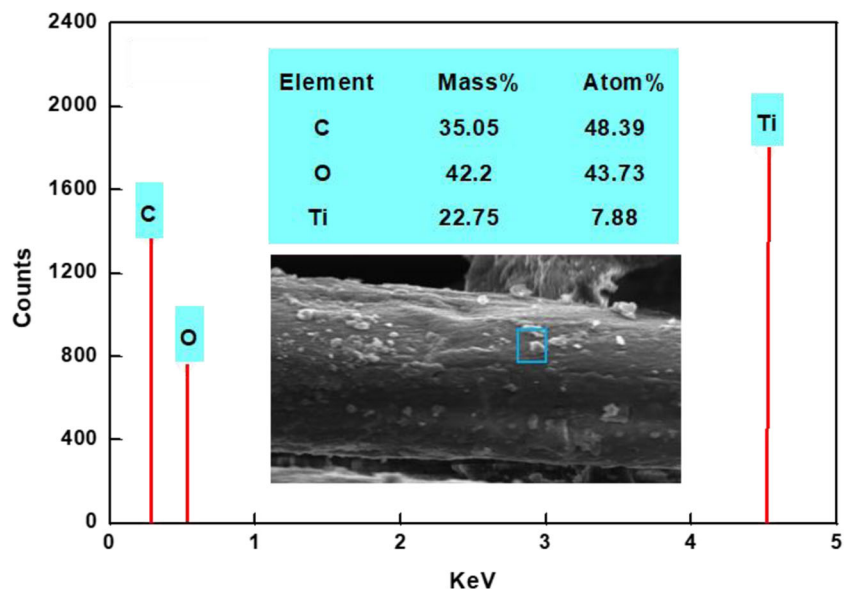
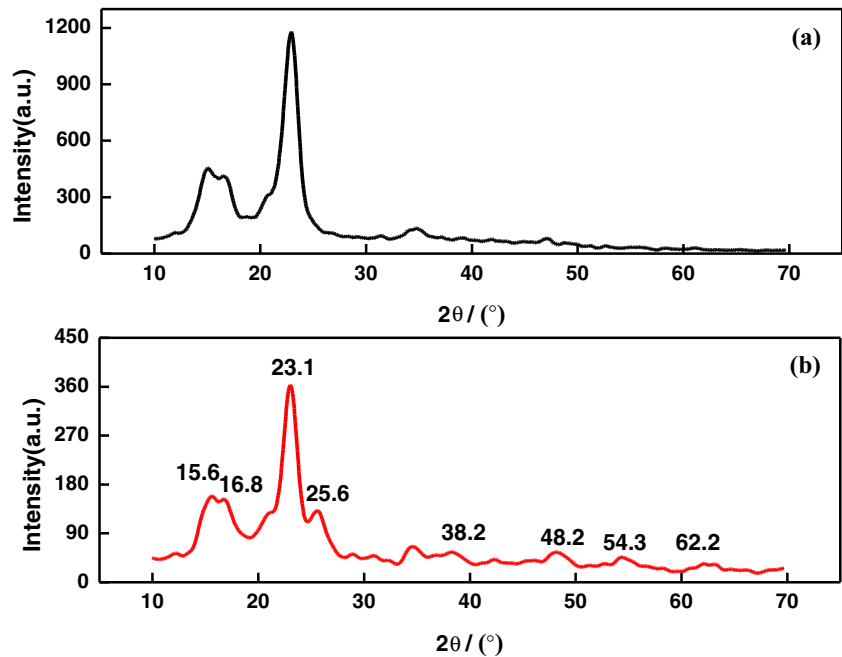


Fig. 5 The XRD patterns of the samples. **a** Pristine CFs. **b** TiO₂/CFs



3.3.2 Effects of TiO₂/CFs Dosage on Photocatalytic Activity

Figure 7 reveals the effects of TiO₂/CFs dosage on photocatalytic performance of TiO₂/CFs under the conditions of UV-365 irradiation for 5 h and MB solution concentration of 10 mg/L. When the dosage of TiO₂/CFs was less than 4.8 g/L, the degradation rate of MB solution increased with the increase of TiO₂/CFs. This was because the more TiO₂/CFs could provide, the more active sites there are and the more dyes could be adsorbed and degraded. However,

when the dosage of TiO₂/CFs exceeded 4.8 g/L, the degradation rate of MB solution did not significantly increase with the addition of TiO₂/CFs. This was because the presence of excess TiO₂/CFs would lead to a decrease in light transmittance, thus limiting the irradiated areas of TiO₂/CFs. Therefore, for this experiment, the optimum dosage of TiO₂/CFs was 4.8 g/L.

3.3.3 Effects of Dye Concentration on Photocatalytic Activity

Figure 8 displays the effects of MB concentration on photocatalytic performance of TiO₂/CFs under the conditions of UV-365 irradiation for 5 h and TiO₂/CFs dosage of 4.8 g/L. As can be seen from Fig. 8, the degradation rate of MB solution decreased with the increase of initial concentration of MB solution. The reason was that when the concentration of MB solution was relatively low, the number of dyes in the solution was relatively small, so there were relatively few dyes migrating and enriching to the TiO₂/CFs surface. However, there were relatively many active sites on the surface of TiO₂/CFs, and fewer dyes were not enough to enable all active sites of TiO₂/CFs to exert the catalytic ability. When the concentration of MB solution was 5 mg/L, the degradation rate of TiO₂/CFs to MB solution was the highest, reaching 98%. With the increase of MB solution concentration, the amount of MB

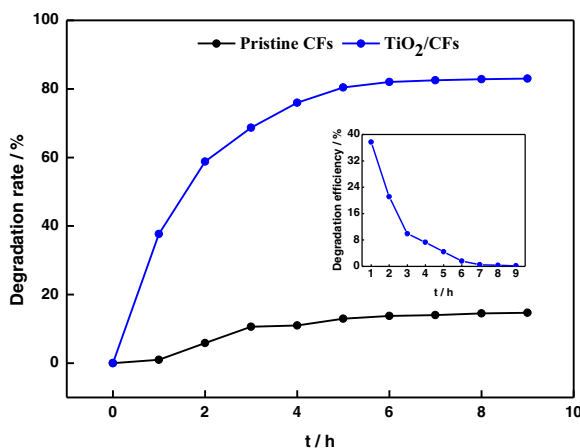


Fig. 6 The effects of illumination time on degradation rate of MB solution under UV-365

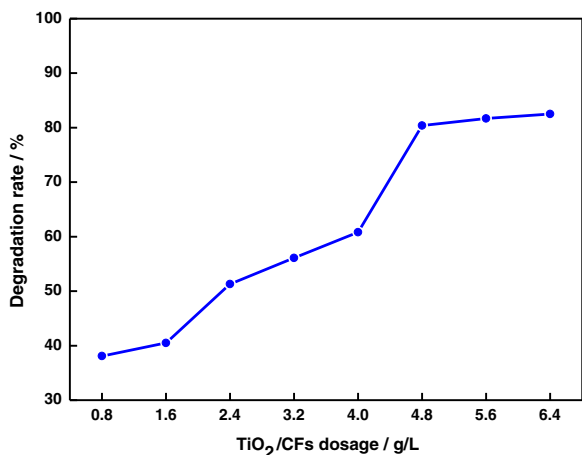


Fig. 7 The effects of TiO₂/CFs dosage on degradation rate of MB solution

adsorbed on the TiO₂/CFs surface gradually reached saturation, and the catalytic capacity also reached maximum. In addition, intermediate products that were difficult to decompose would also accumulate around TiO₂/CFs due to lack of time for reaction, hindering the progress of photocatalytic reaction. Therefore, the prepared TiO₂/CFs were suitable for the degradation of low concentration dyes (5 mg/L, 10 mg/L, and 15 mg/L).

3.3.4 Effects of pH Value on Photocatalytic Activity

Figure 9 describes the effects of initial pH value on photocatalytic performance of TiO₂/CFs under the

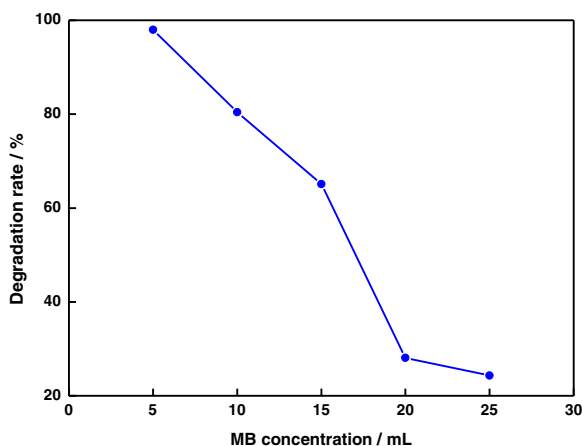


Fig. 8 The effects of dye concentration on degradation rate of MB solution

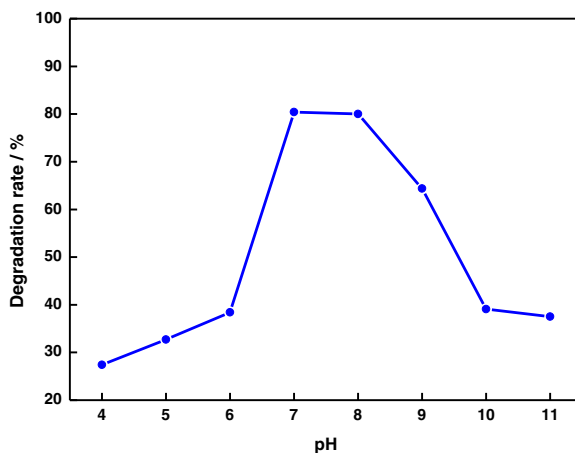


Fig. 9 The effects of the initial pH value on degradation rate of MB solution

conditions of UV-365 irradiation for 5 h, TiO₂/CFs dosage of 4.8 g/L, and MB concentration of 10 mg/L. It could be seen that the degradation of MB by TiO₂/CFs first increased and then decreased with the increase of pH value in the pH range of 4.0–11.0. The isoelectric point of TiO₂ in water was about pH = 6.0 (Devipriya and Yesodharan 2010), which meant that the surface of TiO₂ was neutral. When the solution was pH < 6.0, the TiO₂ surface had a net positive charge, as shown in Eq. (4) (Kaur et al. 2018). Because MB was a cationic dye, the existence of TiOH₂⁺ was not conducive to the adsorption of MB by TiO₂/CFs. So, the degradation of MB by TiO₂/CFs was obviously inhibited under acidic conditions. When the solution was pH > 6.0, the TiO₂ surface carried a net negative charge, as shown in Eq. (5)

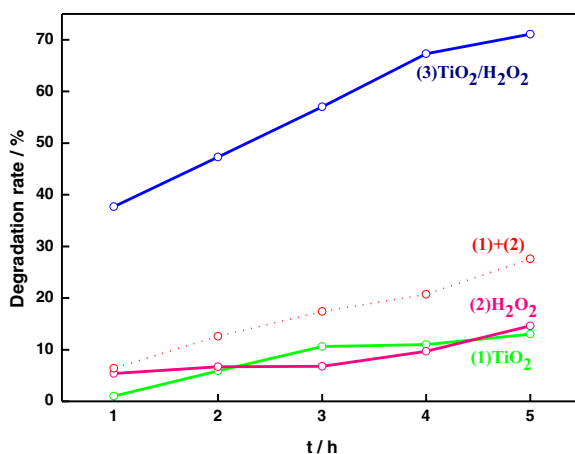
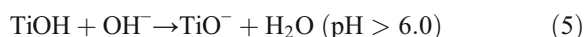


Fig. 10 The degradation rate of MB solution under different conditions

(Kaur et al. 2018). This was also conducive to the migration of holes to the surface of TiO_2 and the formation of $\cdot\text{OH}$ with strong oxidation by reacting with OH^- , H_2O , and other electron donors on the surface of TiO_2 . In addition, TiO_2 was negatively charged in neutral and weakly alkaline solutions and electrostatically adsorbed MB cations (Azeez et al. 2018), thus greatly increasing the degradation of MB. Particularly, when the solution was $\text{pH} = 7.0$, the degradation rate of MB was the highest, up to 80.4%.



However, when the pH the solution was $\text{pH} > 9.0$, the degradation rate of MB solution decreased significantly. To sum up, TiO_2/CFs was more beneficial to the degradation of MB under neutral or weakly alkaline conditions. Since the pH value of MB solution itself was about 7, there was no need to adjust the pH value later.

3.3.5 Effects of H_2O_2 Dosage on Photocatalytic Activity

As a kind of strong oxidative reagent and electron scavenger, the dosage of H_2O_2 is considered to be an important parameter affecting the photocatalytic degradation process because it is directly related to the amount of $\cdot\text{OH}$ generated in the photocatalytic reaction.

First of all, in order to prove that H_2O_2 could promote TiO_2 to degrade dyes, three experiments were designed as shown in Fig. 10. The curve (1) showed the degradation rate of MB solution only in the presence of TiO_2/CFs . The curve (2) showed the degradation rate of MB solution only in the presence of H_2O_2 . The dashed line (1)+(2) was the sum of the degradation rates of MB solution under conditions (1) and (2) alone. The curve (3) showed the degradation of MB solution in the presence of TiO_2/CFs and H_2O_2 . As can be seen from Fig. 11, the degradation rate was obviously (3) > (1) + (2). Therefore, it came to a conclusion that H_2O_2 could promote TiO_2 to degrade dyes.

Subsequently, the effects of H_2O_2 dosage on photocatalytic performance of TiO_2/CFs under the conditions of UV-365 irradiation for 2 h and 4 h, TiO_2/CFs dosage of 4.8 g/L, MB concentration of 10 mg/L, and initial pH value of 7 were discussed, as shown in Fig. 11.

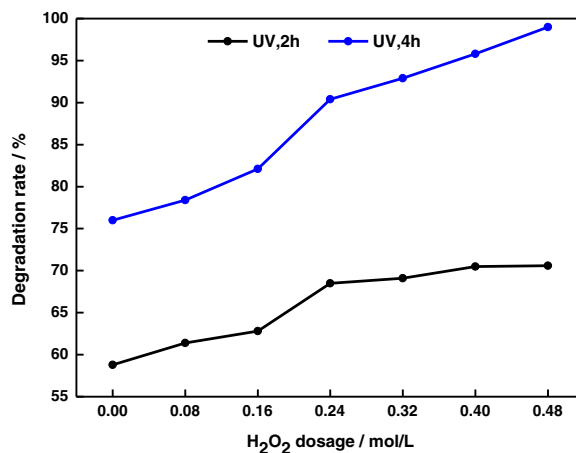


Fig. 11 The effects of H_2O_2 dosage on degradation rate of MB solution

According to the curve of illumination for 2 h (sealed), it could be concluded that in the presence of H_2O_2 , the degradation rate of MB solution first increased and then tended to be stable with the increase of H_2O_2 dosage; the degradation efficiency of MB solution was the highest when 0.24 mol/L H_2O_2 was added to 60 mL MB solution. This was because when the dosage of added H_2O_2 was less than 0.24 mol/L, H_2O_2 could capture electrons on the surface of TiO_2 (Eq. (6)), thus reducing the probability of electron-hole recombination and improving hole utilization (Eq. (7) and Eq. (8)) (Akpan and Hameed 2009). In addition, H_2O_2 may be decomposed directly to generate $\cdot\text{OH}$ under UV irradiation (Eq. (9)) (Navarro et al. 2005), which was the strongest oxidant in aqueous phase systems and could degrade dyes into harmless products (Eq. (10) and Eq. (11)) such as CO_2 and H_2O . When the dosage of added H_2O_2 was above

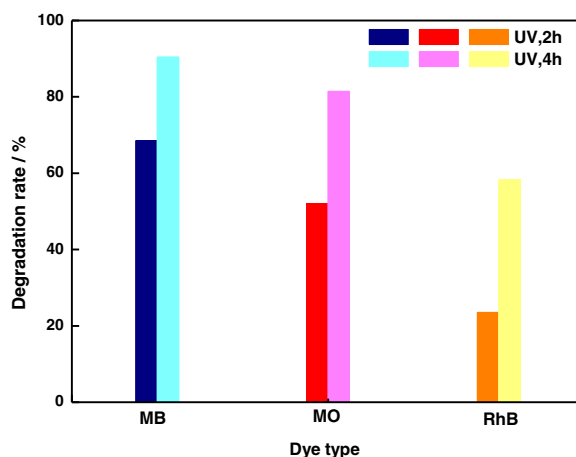
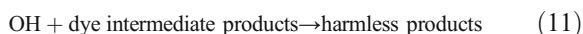
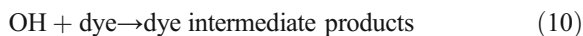


Fig. 12 The effects of dye type on degradation rate

0.24 mol/L, H_2O_2 made quenching reaction due to excess, i.e., H_2O_2 reacted with $\cdot\text{OH}$ to form $\cdot\text{OOH}$ (Eq. (12)) and the reaction (Eq. (13)) (Fayazi et al. 2016), thus reducing the degradation efficiency.



According to the curve of illumination for 4 h (unsealed), it could be seen that the degradation rate of MB solution kept increasing obviously with the increase of H_2O_2 dosage. This may be because the opening of the preservative film after 2 h of light would bring in air and promote the photocatalytic degradation.

Therefore, in the following work of this experiment, when studying the effect of UV-365 and H_2O_2 on other dyes, the optimal H_2O_2 dosage was 0.24 mol/L.

3.3.6 Degradation Effect of TiO_2/CFs on Different Dyes

Figure 12 presents the effects of dye type on photocatalytic performance of TiO_2/CFs under the conditions of UV-365 irradiation for 2 h and 4 h, TiO_2/CFs dosage of 4.8 g/L, dye concentration of 10 mg/L, initial pH value of 7, and H_2O_2 dosage of 0.24 mol/L. The degradation rates of MB, MO, and RhB were 68.5%, 52.0%, and 23.5%, respectively, when the irradiation time was 2 h (sealed). The degradation rate increased by 20–30% to 90.4%, 81.4%, and 58.3% when the illumination time was further extended to 4 h (unsealed). Therefore, the

prepared TiO_2/CFs not only had excellent degradation effect on MB but also had certain degradation effect on MO and RhB.

4 Conclusion

Anatase TiO_2 was synthesized with uniform distribution and firm loaded in situ with CFs as carrier and TBT as raw material by the hydrothermal method and low-temperature calcination. Therefore, the excellent photocatalytic performance of nano- TiO_2 permanently endowed CFs. The photocatalytic properties of the prepared TiO_2/CFs were tested by visible spectrophotometry. The results showed that TiO_2/CFs had good degradation effects on MB, MO, and RhB. The degradation rates of MB, MO, and RhB were 90.4%, 81.4%, and 58.3%, separately, at TiO_2/CFs dosage of 4.8 g/L, initial dye concentration of 10 mg/L, pH of 7, and H_2O_2 dosage of 0.24 mol/L, after 4 h of UV-365 irradiation.

Funding Information The authors acknowledge the Scientific Research Fund of Taiyuan University of Technology for financial support (Project No. 20504020203) and Shanxi Provincial Foundation for Returned Scholars, China (Project No. 2017048).

References

- Akpan, U. G., & Hameed, B. H. (2009). Parameters affecting the photocatalytic degradation of dyes using TiO_2 -based photocatalysts: a review. *Journal of Hazardous Materials*, 170, 520–529.
- Azeez, F., Al-Hetlani, E., Arafa, M., et al. (2018). The effect of surface charge on photocatalytic degradation of methylene blue dye using chargeable titania nanoparticles. *Sci Rep-UK*, 8, 7104.
- Cai, L. J., Li, Y. W., Li, Y. H., et al. (2018). Synthesis of zincphthalocyanine-based conjugated microporous polymers with rigid-linker as novel and green heterogeneous photocatalysts. *Journal of Hazardous Materials*, 348, 47–55.
- Das, D., Sabaraya, I. V., Zhu, T., et al. (2018). Aggregation behavior of multiwalled carbon nanotube-titanium dioxide nanohybrids: probing the part-whole question. *Environmental Science & Technology*, 52, 8233–8241.
- Devipriya, S. P., & Yesodharan, S. (2010). Photocatalytic degradation of phenol in water using TiO_2 and ZnO. *Journal of Environmental Biology*, 31, 247–249.
- Fayazi, M., Taher, M. A., Afzali, D., et al. (2016). Enhanced Fenton-like degradation of methylene blue by magnetically activated carbon/hydrogen peroxide with hydroxylamine as Fenton enhancer. *Journal of Molecular Liquids*, 216, 781–787.

- Giesz, P., Celichowski, G., Puchowicz, D., et al. (2016). Microwave-assisted TiO₂: anatase formation on cotton and viscose fabric surfaces. *Cellulose*, 23, 2143–2159.
- Goudarzi, V., & Shahabi-Ghahfarrokhi, I. (2018). Photoproducible and photo-degradable starch/TiO₂ bionanocomposite as a food packaging material: development and characterization. *International Journal of Biological Macromolecules*, 106, 661–669.
- John, N., Tharayil, N. J., & Somaraj, M. (2017). Photocatalytic degradation of methyl orange using biologically enhanced tin oxide nanoparticles under UV-irradiation. *Journal of Materials Science: Materials in Electronics*, 28, 5860–5865.
- Kaur, H., Kumar, S., Verma, N. K., et al. (2018). Role of pH on the photocatalytic activity of TiO₂ tailored by W/T mole ratio. *Journal of Materials Science: Materials in Electronics*, 29, 16120–16135.
- Kinsinger, N., Tantuccio, A., Sun, M. W., et al. (2011). Photocatalytic titanium dioxide composite. *Journal of Nanoscience and Nanotechnology*, 11, 7015–7021.
- Liang, Y., Zhou, B., Li, N., et al. (2018). Enhanced dye photocatalysis and recycling abilities of semi-wrapped TiO₂@carbon nanofibers formed via foaming agent driving. *Ceramics International*, 44(2), 1711–1718.
- Liu, X. H., Liu, Y., Lu, S. Y., et al. (2018). Performance and mechanism into TiO₂/zeolite composites for sulfadiazine adsorption and photodegradation. *Chemical Engineering Journal*, 350, 131–147.
- Ma, J., Liu, Y., Ali, O., et al. (2018). Fast adsorption of heavy metal ions by waste cotton fabrics based double network hydrogel and influencing factors insight. *Journal of Hazardous Materials*, 344, 1034–1042.
- Mishra, A., & Butola, B. S. (2017). Deposition of Ag doped TiO₂ on cotton fabric for wash durable UV protective and antibacterial properties at very low silver concentration. *Cellulose*, 24, 3555–3571.
- Navarro, P., Sarasa, J., Sierra, D., et al. (2005). Degradation of wine industry wastewaters by photocatalytic advanced oxidation. *Water Science and Technology*, 51, 113–120.
- Pensupa, N., Leu, S. Y., Hu, Y., et al. (2017). Recent trends in sustainable textile waste recycling methods: current situation and future prospects. *Topics in Current Chemistry*, 375, 76.
- Phaltane, S. A., Vanalakar, S. A., Bhat, T. S., et al. (2017). Photocatalytic degradation of methylene blue by hydrothermally synthesized CZTS nanoparticles. *Journal of Materials Science: Materials in Electronics*, 28, 8186–8191.
- Rauf, M. A., Meetani, M. A., & Hisaindee, S. (2011). An overview on the photocatalytic degradation of azo dyes in the presence of TiO₂ doped with selective transition metals. *Desalination*, 276, 13–27.
- Sosnov, E. A., Trubina, T. S., & Malygin, A. A. (2017). Chemical assembly of a titanium oxide layer on microporous silica. *Russian Journal of General Chemistry*, 87, 1786–1793.
- Sun, Y. P., Guduru, R., Lin, F., et al. (2000). Preparation of nanoscale semiconductors through the rapid expansion of supercritical solution (RESS) into liquid solution. *Industrial and Engineering Chemistry Research*, 39, 4663–4669.
- Tang, H. W., Ng, K. M., Chui, S. S. Y., et al. (2009). Analysis of melamine cyanurate in urine using matrix-assisted laser desorption/ionization mass spectrometry. *Analytical Chemistry*, 81, 3676–3682.
- Vukoje, I., Kovač, T., Džunuzović, J. V., et al. (2016). Photocatalytic ability of visible-light-responsive TiO₂ nanoparticles. *Journal of Physical Chemistry C*, 120, 18560–18569.
- Wang, W. J., Huang, G. C., Yu, J. C., et al. (2015). Advances in photocatalytic disinfection of bacteria: development of photocatalysts and mechanisms. *Journal of Environmental Sciences (China)*, 34, 232–247.
- Wu, D. Y., & Long, M. C. (2011). Realizing visible-light-induced self-cleaning property of cotton through coating N-TiO₂ film and loading AgI particles. *ACS Applied Materials & Interfaces*, 3, 4770–4774.
- Xu, Z., Li, X., Wang, W., et al. (2016a). Microstructure and photocatalytic activity of electrospun carbon nanofibers decorated by TiO₂ nanoparticles from hydrothermal reaction/blended spinning. *Ceramics International*, 42(13), 15012–15022.
- Xu, Z., Wu, T., Shi, J., et al. (2016b). Photocatalytic antifouling PVDF ultrafiltration membranes based on synergy of graphene oxide and TiO₂ for water treatment. *Journal of Membrane Science*, 520, 281–293.
- Yang, M. P., Liu, W. Q., Jiang, C., et al. (2019). Robust fabrication of superhydrophobic and photocatalytic self-cleaning cotton textile based on TiO₂ and fluoroalkylsilane. *Journal of Materials Science*, 54, 2079–2092.
- Yusoff, M. M., Mamat, M. H., Malek, M. F., et al. (2016). Growth of titanium dioxide nanorod arrays through the aqueous chemical route under a novel and facile low-cost method. *Materials Letters*, 164, 294–298.
- Zhang, H., & Yang, L. (2012). Immobilization of nanoparticle titanium dioxide membrane on polyamide fabric by low temperature hydrothermal method. *Thin Solid Films*, 520, 5922–5927.
- Zhang, B., Maimaiti, H., Zhang, D. D., et al. (2017). Preparation of coal-based C-dots/TiO₂ and its visible-light photocatalytic characteristics for degradation of pulping black liquor. *Journal of Photochemistry and Photobiology A*, 345, 54–62.
- Zhou, W. Y., Zhang, Y. Y., & Shi, Y. D. (2017). In situ loading TiO₂ and its photocatalysis and UV resistance on cotton fabric. *Fibers and Polymers*, 18, 1073–1078.

Publisher's Note Springer Nature remains neutral with regard to jurisdictional claims in published maps and institutional affiliations.